NOVEL METHOD FOR MEASURING 3-D NANOMETER SCALE VIBRATIONAL

MOTION USING OPTICAL COHERENCE TOMOGRAPHY

A Thesis

by

PETRAL ABONGYA ABONG

Submitted to the Jackson College of Graduate Studies of the
University of Central Oklahoma
in partial fulfillment of the requirements for the degree of

MASTER OF SCIENCE

Chair of Committee,	Scott P. Mattison
Committee Members,	Weldon J. Wilson
	Mohamed Bingabr
Chair of Department,	Charles Hughes

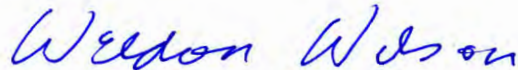
December 2019

Major Subject: Engineering Physics-Physics

Novel Method for Measuring 3-D Nanometer Scale Vibrational Motion Using Optical Coherence Tomography
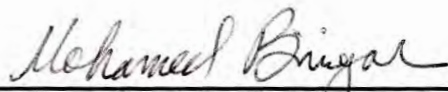
Thesis Approved:

_____

Dr. Scott Mattison, Committee Chair

_____

Dr. Weldon Wilson, Committee Member

_____

Dr. Mohamed Bingabr, Committee Member

ABSTRACT

Optical Coherence Tomography(OCT) is a non-invasive diagnostic technique capable of providing structural information millimeters deep in tissue. In recent years, OCT has been widely adopted as a clinical diagnostic tool in ophthalmology and is becoming a relevant tool in the field of otolaryngology. Optical Coherence Vibrometry (OCV), a specialized approach to OCT, has been demonstrated as a powerful tool for quantifying vibrational motion. OCV is based on the fundamental physical principles of Doppler OCT, meaning OCV is a computationally intensive technique and all measurements are dependent upon the Doppler angle. The goal of this research project is to provide a novel approach to vibrational sensing via OCT that may be used in combination with OCV to accurately measure total vibrational motion independent of the Doppler angle. This thesis presents a new approach to measuring vibrational motion by combining speckle variance and Doppler OCT. Speckle present in biological tissue imaging is due to the interference of light backscattered from the tissue. Generally considered a source of noise, speckle carries information about the tissue microstructure (or test sample). In this new approach, Speckle provides the measurement of the bulk vibrational motion (motion of the entire system) while, the magnitude of vibration taken from phase measurements is used to characterize the magnitude of vibration from speckle.

DEDICATION

This piece of work is dedicated to Mr./Mrs. John Hebblethwaite for their prayers and unending support during the realization of this project.

ACKNOWLEDGEMENTS

CONTRIBUTORS AND FUNDING SOURCES

Contributors

This work was supervised by a thesis committee consisting of Dr Scott Mattison[Advisor], Dr Weldon Wilson and Dr Mohamed Bingabr of the Department of Engineering and Physics at the University of Central Oklahoma

Funding Sources

NOMENCLATURE

OCT	Optical Coherence Tomography
OCV	Optical Coherence Vibrometry
XCT	X-ray Computed Tomography
MRI	Magnetic Resonance Imaging
LDV	Laser Doppler Vibrometry
AFM	Atomic Force Microscopy
DVU	Doppler Vibrometry Ultrasound
TD-OCT	Time domain Optical Coherence Tomography
FD-OCT	Fourier Domain Optical Coherence Tomography
SLD	Superluminescent Diode
FOI	Fiber Optic Isolator
LED	Light Emitting Diode

TABLE OF CONTENTS

LIST OF FIGURES

X

LIST OF TABLES

CHAPTER 1

INTRODUCTION

1.1 Purpose of Study

The main purpose of this study is to develop and characterize a novel method for the direct measurement of nanometer scale 3-D vibrational motion using Optical Coherence Tomography(OCT).

1.2 Statement of the Hypothesis/Research Question

We hypothesize that combining speckle variance and Doppler phase OCT, we will be able to directly measure vibrational motion down to one nanometer using optical coherence tomography (OCT). The research question we are asking is this: Will speckle variance provide vibrational motion that is independent of Doppler angle?

1.3 Significance of the Study

The current standard for quantifying vibrational motion is laser Doppler vibrometry (LDV). LDV is capable of quantifying picometer scale vibrational motion from a single surface. In recent years, many groups have demonstrated Optical Coherence Vibrometry (OCV) to be a powerful tool for measuring vibrational motion in layered samples. Based on the concepts of low coherence interferometry and Doppler imaging, OCV may isolate vibrational motion on the order of tens of picometers across multiple layers of samples. The primary drawback to both techniques is their dependence on the Doppler angle, as such; the bulk motion of the entire system cannot be measured. This research proposes a new method for measuring vibrational motion down to a nanometer scale by combining speckle variance and Doppler OCT. We propose utilizing speckle variance of an OCT

imaging system to quantify the bulk motion of the entire system. Due to the properties of speckle, we believe the measured vibrational magnitude should be independent of Doppler angle. The ability to isolate bulk vibrational magnitude of a sample would open new avenues of research in the field of vibrometry, especially in the field of hearing loss.

1.4 Definitions

1.4.1 Optical Coherence Tomography

Optical Coherence Tomography (OCT) OCT is a non-invasive diagnostic technique capable of providing structural information millimeters deep in tissue. OCT uses low coherence interferometry to produce a 2-D image of optical scattering from the internal tissue microstructures in a way that is analogous to ultrasonic pulse-echo imaging

1.4.2 Speckle

Speckle is a source of noise in all imaging systems that utilizes a coherent light source. In its simplest form, speckle may be interference between wave fronts of a planar wave as they scatter off a rough sample. While speckle is generally considered to be a source of noise in biological tissues, it also carries information about sample motion, microstructure, and surface roughness.

1.5 Delimitations, Limitations, and Assumptions

We are currently developing and verifying a novel approach for detecting vibrations using optical coherence tomography. Our current testing technique is utilizing a single piezo element and looking at just the surface of this device. OCT as a technique is optimal for layered structures; however, our current tests ignore the challenges and benefits of imaging structures that are multilayered.

Furthermore, we are assuming that phase sensitive OCT provides accurate and precise measurements of displacement for vibrations occurring in parallel with the laser excitation pathway and that our piezo is providing repeatable displacements regardless of orientation.

CHAPTER 2

LITERATURE REVIEW

2.1 Imaging modalities

There are many different imaging techniques that have been discovered over the years, some of which include, X-ray computed Tomography(XCT), Magnetic Resonance Imaging (MRI), Confocal microscopy, ultrasound and so on. The figure below gives a comparison between the various methods for imaging biological tissues.
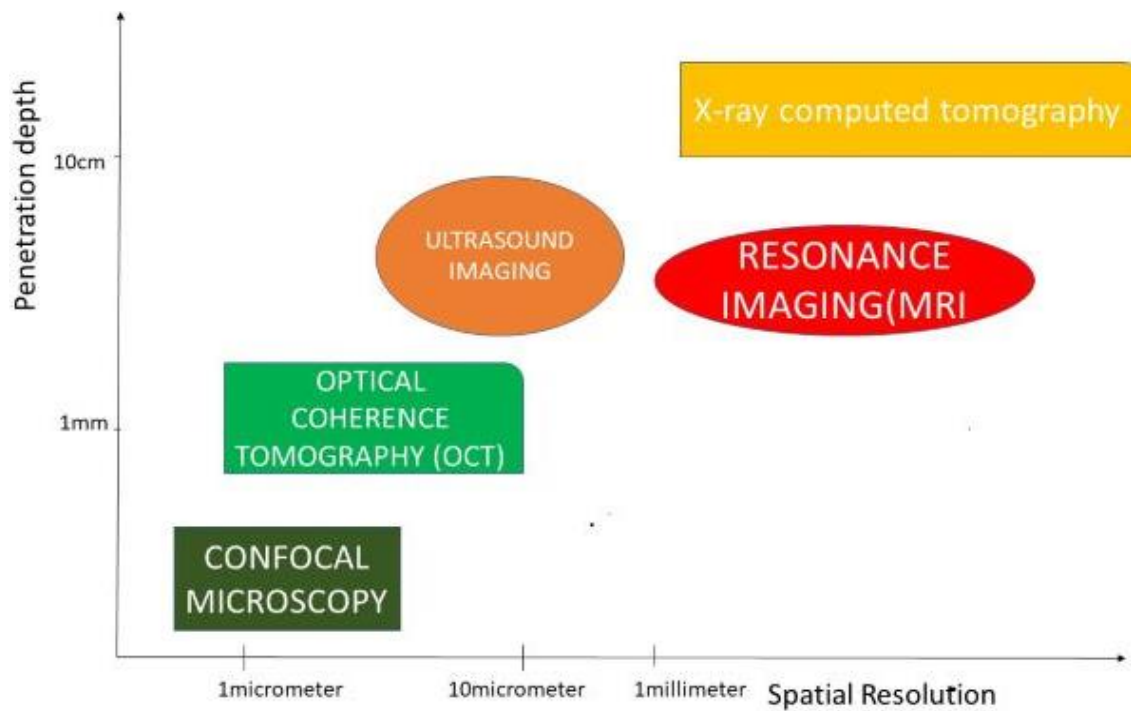
Figure 1 Graph of Penetration depth vs Spatial Resolution for various imaging techniques, [7, p. 3]

Using **X-ray computed tomography (XCT),** it is possible to provide images of the inner and middle ear bony features at a 500 microns resolution, however, some deformations of the bone and soft tissue of the cochlear are not readily visible[2].

Magnetic resonance imaging (MRI) can provide imaging of the soft structures of the inner and middle ear but its resolution is limited to 1mm for most commercial systems [3].

Confocal microscopy is an optical imaging technique with very high resolution approaching 1 micrometer but is limited by the diffraction of light. However, Confocal microscopy has a very poor penetration power due to optical scattering. Experiments using confocal microscopy for imaging biological tissues has attained only a few hundred micrometer of depth, making it unsuitable for applications where significant imaging depth is required.[7, p.3]

Ultrasound is analogous to OCT, while ultrasound uses sound as a key component for imaging, OCT uses light. Ultrasound can provide very high depths of up to 10 centimeters due to low attenuation of sounds at low frequencies within the range of clinical applications.[7, p.3]. Ultrasound can achieve resolution down to the scale of OCT if performed properly.

In addition to the disadvantages of the various methods above, none of these approaches have the required speed to image the dynamic processes that occur in the middle and inner ear and most of these traditional methods lack the resolution needed to image anything other than gross malformations of the organs and are not well suited for measuring vibratory function.

OCT bridges the gap between the higher-resolution optical imaging technologies, such as confocal reflectance microscopy, and the lower resolution clinical technologies, such as X-ray CT and MRI[7, p.4]. Furthermore, OCT has specific advantages such as its high depth and transverse resolution which makes it possible to measure periodic, nanometer scale mechanical motion observed in the vocal cords, middle and inner ear[2]. OCT is contact free and minimally invasive (Unlike surgical operations) and has the possibility of creating various functional dependent images. The combination of resolution and the ability to do functional vibratory imaging makes OCT a powerful tool for imaging and vibrational studies.

The prevalence of hearing loss in the US and in the globe as a whole is growing quickly especially in children under 3 years old [4]and also in adults over 18 years. This prevalence increases with age and has the highest impact on adults above 60 years[5]. It is imperative to carry out research on the aspect of hearing loss and provide better methods or techniques to help eradicate this prevalence.

This research serves as a base through which other research on hearing will spring forth. Measuring significant changes in the vibrations of an object(in this case a piezo) using speckle variance and doppler OCT, can be used in the future to study vibrational mechanics in rodents and eventually humans. It is my projection that, in the long run, this research will play a key role in combatting hearing loss in humans.

2.2 Nano-scale vibrational motion

Over the years many different methods have been introduced to detect Nano-scale vibrations. Understanding the functionalities of vibrational motion can be applicable in many fields in science, such as medicine and biomedical engineering. Studying the vibrational mechanics of the ear is an ongoing process and is fundamental to finding remedies to hearing loss.

Buried deep within the middle and inner ear of humans is the cochlea. The cochlea is a spiraled, hollow, conical chamber of bone in which waves propagate from the base (near the middle ear and the oval window) to the apex (the top or center of the spiral). The cochlea is the part of the inner ear involved in hearing, it houses the organ responsible for the transduction of sound into electrical impulses in the brain. When sound waves reach the inner ear, the cochlea receives the sound waves in the form of vibrations through the oval window. The vibrations cause precise, localized motion within the cochlea and complex interactions between components of the inner ear transduce the vibrational motion into electrical impulses, which the brain interprets. When damage occurs to components of the inner ear, small changes occur in the healthy vibrational response to sound. These small changes have a drastic impact on the ability of the inner ear to detect sound.

As the cochlea is located deep within bone and involves the interaction of soft tissue component on a cellular level, vibrational mechanics has been historically difficult to study. In this section, I will introduce four different methods for detecting Nano-scale vibrations but will focus on OCT Vibrometry because it holds promise for this study.

7

2.2.1. Laser doppler vibrometry(LDV)

Laser doppler vibrometry (LDV) is a technique for measuring non-contact vibrations of a surface using a laser doppler vibrometer. The vibrometer is generally a two-beam laser interferometer which measures the frequency or phase differences between an internal reference beam and a test beam. The beam from the laser with frequency f_0 divides into a reference beam and a test beam when it strikes the beam splitter. The test beam passes through the Bragg cell and a frequency shift fb is added to it. The frequency shift beam is directed to the sample; the motion of the sample adds a doppler shift to the beam given by equation 1 below

$$f_d = 2*v(t)*cos(\alpha)/\lambda \ (1)$$

where λ is the wavelength of the light, $v(t)$ is the velocity of the sample as a function of time and α is the angle between the laser beam and the velocity vector. When the light strikes the sample, it is scattered into different direction, and some of the scattered light with frequency $f_0 + f_b + f_d$ is collected by the laser doppler vibrometer and is reflected by the beam splitter into the photodetector.
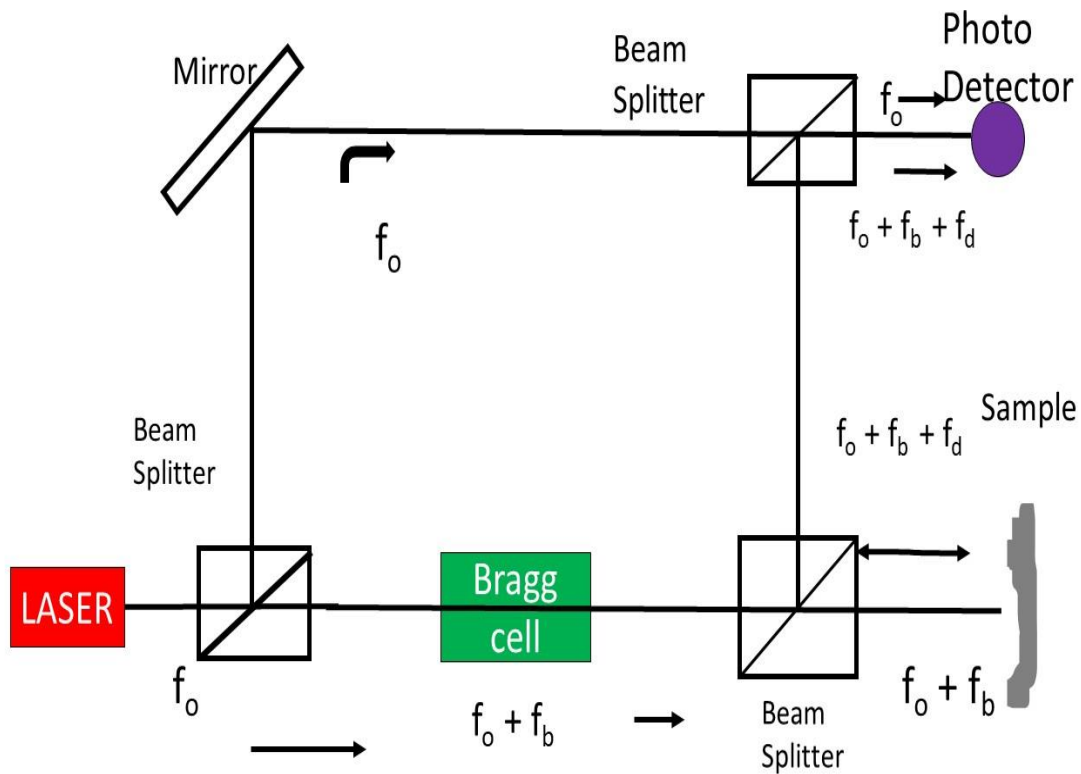
Figure 2 Schematic of a laser doppler vibrometer

The scattered light is recombined with the reference beam at the photodetector. The detector responds to the difference in the frequency of the 2 lights fb + fd . The output of the detector is a frequency modulated signal, with the Bragg cell frequency as the carrier frequency and the Doppler shift as the modulation frequency. This signal can be demodulated to derive the velocity or displacement of the vibrating sample. Information about the velocity of the vibrating sample will help us understand how the sample vibrates. LDV has been used in different applications in Medicine and other fields.

Goode et al, used the laser doppler system clinically for measurement of the tympanic membrane(TM), malleus and prosthesis head displacement in response to sound inputs of 80dB to 100dB sound pressure levels(SPL)[6]. The results of their research help provide otologist with knowledge of the TM and ossicular functions that was unique in evaluating middle ear function.

Stasche et al, measured vibrations in the tympanic membrane of the middle ear using laser doppler vibrometry, they were able to find a correlation between the umbo and the experimentally produced middle ear disorder.[7]

John J Rosowski *et al* were able to use laser doppler vibrometry to investigate the relationship between the sound induced velocity of the tympanic membrane at the umbo and the cause of conductive hearing loss when the tympanic membrane was normal, and the middle ear was aerated. They found out that the pattern of laser doppler vibrometry measurements in post stapedectomy approximated the patterns in ears of ossicular interruptions. They concluded that laser doppler vibrometry is a useful tool for investigating middle ear function[8].

A. Nuttall *et al* measured vibrations of the Basilar Membrane (BM) using LDV. They were able to get frequency tuning curves and input/output intensity functions.[9]

S Terasaki *et al* in their article "Nondestructive Measurement of Kiwifruit Ripeness using Laser Doppler Vibrometry", used an LDV to evaluate viscoelastic properties of kiwifruit at different stages of ripeness. In their measurement they deduced a relationship between

the stiffness coefficient and the loss coefficient. They found that early stages of fruit softening are reflected by the stiffness coefficient and late stages are reflected by the loss coefficient[10].

2.2.2 Atomic Force Microscopy(AFM)

AFM is a high-resolution scanning probe microscope with very high resolution up to nanometer scale. First discovered by Binning and Rohrer in 1986[11], the AFM consists of a cantilever with a sharp probe that scans through the surface of the test sample. When the tip of the probe is brought very close to the test sample, the forces between the tip of the probe and the sample cause a deflection in the cantilever. The deflection in the cantilever causes the laser beam that fall on it to be reflected onto a photodiode. The variation of the laser beam is a measure of the applied forces.
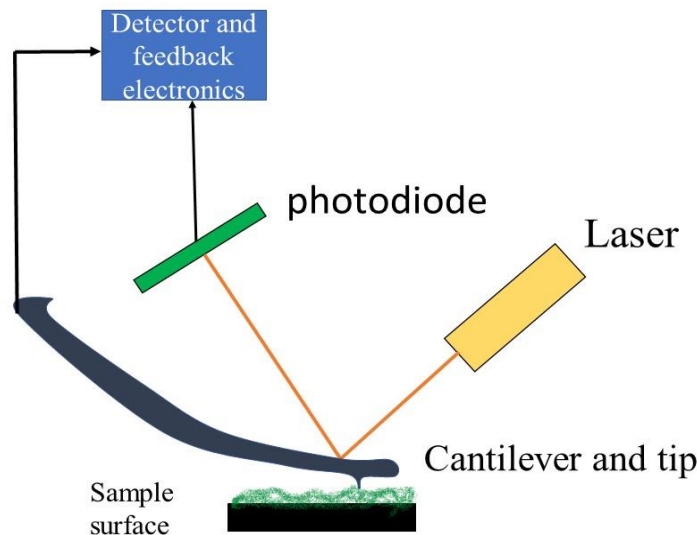
Figure 3 Schematic Principle for the AFM

Two primary modes of operation exist for conducting AFM- contact and non-contact mode.

In contact mode, the tip of the probe of the cantilever drags through the surface of the test sample, and the deflection of the cantilever is used to measure the contours of the surface. Noise and drift that can affect the signal is eliminated by using a low stiffness cantilever, but this allows the attractive forces to pull the tip to the surface of the sample. To avoid this the tip is in contact with the surface of the sample where the overall forces is repulsive.

In non-contact mode, the tip of the probe vibrates slightly above its resonant frequency without it touching the test sample. A feedback loop system helps to maintain the oscillation amplitude constant by changing the distance from the test sample to the tip of the probe. Recording the distance between the tip and the sample at each point enable the software to construct a topographic image of the test sample.

The AFM can measure a very small sample with a very high level of accuracy, and it does not require to be used in a vacuum as other technologies, and the sample does not need to undergo any treatment.

The downside of the AFM is the single scan image size, which is of the order of 150*150 micrometers compared with millimeter for a scanning electron microscope. Another disadvantage is its very slow scan time which can lead to a damage in the test sample.

AFM has been used by scientist all over the world for different applications. AFM has been used for doing non-destructive surface profilometry[12], a method that is much needed by most Biologist and as an PEM fuel cell diagnostic tool[13]

2.2.3 Doppler vibrometry ultrasound(DVU)

Doppler Vibrometry ultrasound operates on the principle of doppler effect. The principle of doppler effect explains that sound pitch increases as the source of the sound moves towards the listener and decreases when the source of the sound moves away from the listener. Ultrasound pulses are transmitted into a moving target or sample and backscattered echoes from the vibrating surface is frequency modulated as a result of the doppler effect. The modulated echo or ultrasound signal is received by the transducer that is co-located at the transmitter and processed for information. This method has been used in various fields, especially in the medical field. Sirdar et al introduced ultrasonic doppler vibrometry as a novel method for the detection of left ventricle wall vibrations cause by post-stenotic coronary blood flow[14] and used it to detect coronary artery disease(CAD)[15]. Doppler vibrometry ultrasound has also been used to extract velocity from a walking human body[16] and to study human motion[17]

2.2.4 Optical Coherence Tomography Vibrometry

Optical coherence tomography is imaging of tissues by sections or slices (tomography) using the coherent properties of light. We can study vibrational motion of various biological tissues by imaging the various tissues using the technique of OCT. The image acquired can be and is presently performed in real time using software like MATLAB, to

find every information about the tissues or vibrating object. This can be very beneficial in the long run since predictions could be made and a better model for hearing loss could be created. The principle of OCT is based off of low coherence interferometry.

Low Coherence interferometry

In low coherence interferometry, an interferometer is used with a broadband light source. Light from the light source is split into two by the beam splitter- one goes into the sample and is reflected on the same path in the opposite direction and the other goes to the reference arm and is reflected by the reflecting mirror back in the same path in the opposite direction. They later recombine by means of interference before entering the detector for signal to be processed. Interference occurs when the length from the source to the sample arm matches that from the source and the reference arm.[7, p.7]
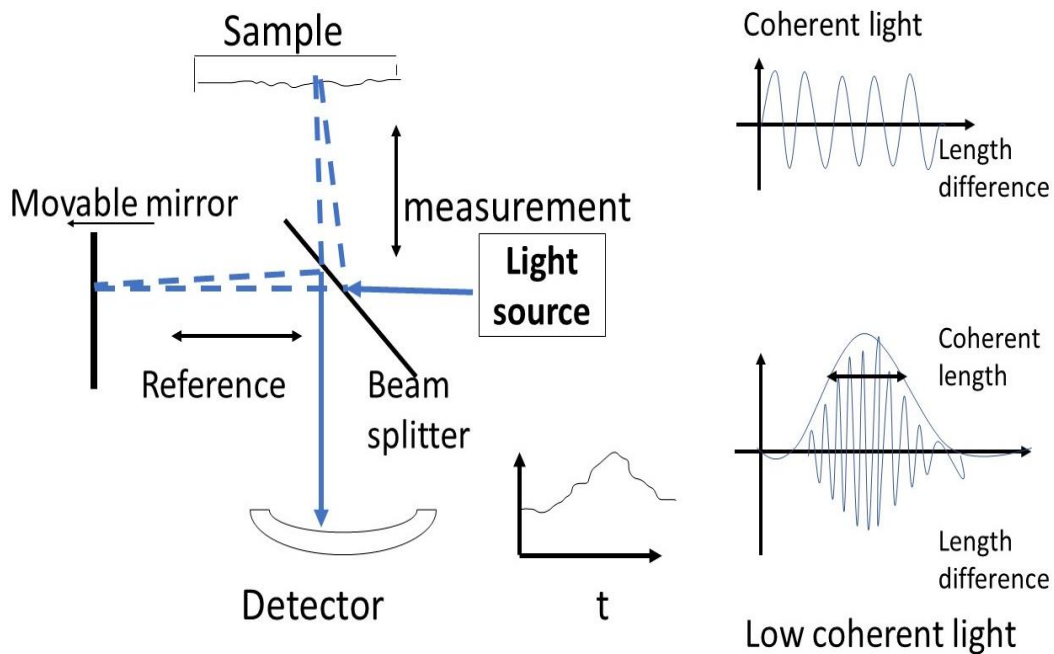
Figure 4 Principle of Low coherence interferometry[7, p.8]

14

Free Optics OCT System

From the figure below, light from the laser source is directed into a beam splitter and it splits into a reference and sample arm by a 50/50 ratio. The light from the sample arm is reflected to the sample and bounces off of the sample and back into the sample arm with different time delays according to the microstructure of the sample arm.
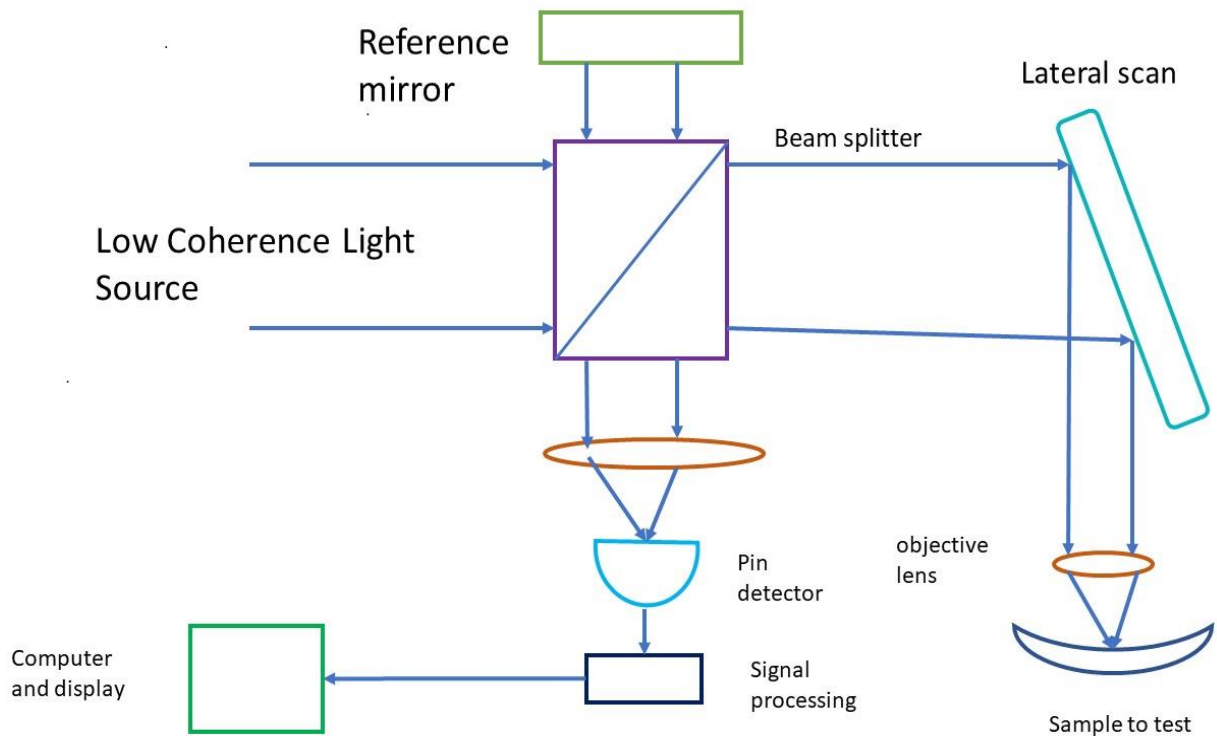
Figure 5 General OCT system for free optics

The light that enters the reference arm is reflected from the reference mirror at a variable distance producing a variable time delay. The light from the sample later interfere constructively with the light from the reference and is detected by the detector, which is usually a photodiode that measures the intensity of the interfering beams of light.

15

Fiber Optics OCT system

 The implementation of the optical fiber in OCT gives the possibility of altering the ratio of the amount of light that goes to the reference arm and sample arm. As light from the laser or photodiode enters the Fiber-coupler and is split in two, part of the light goes to the reference arm and is reflected through that same part, and the other bounces off the sample and back into the Fibre-coupler. The two reflected light beams recombines by means of interference and is detected. The Fiber optics implementation of OCT produces an image of very high resolution, since it is possible to change the amount of light that goes to the sample.
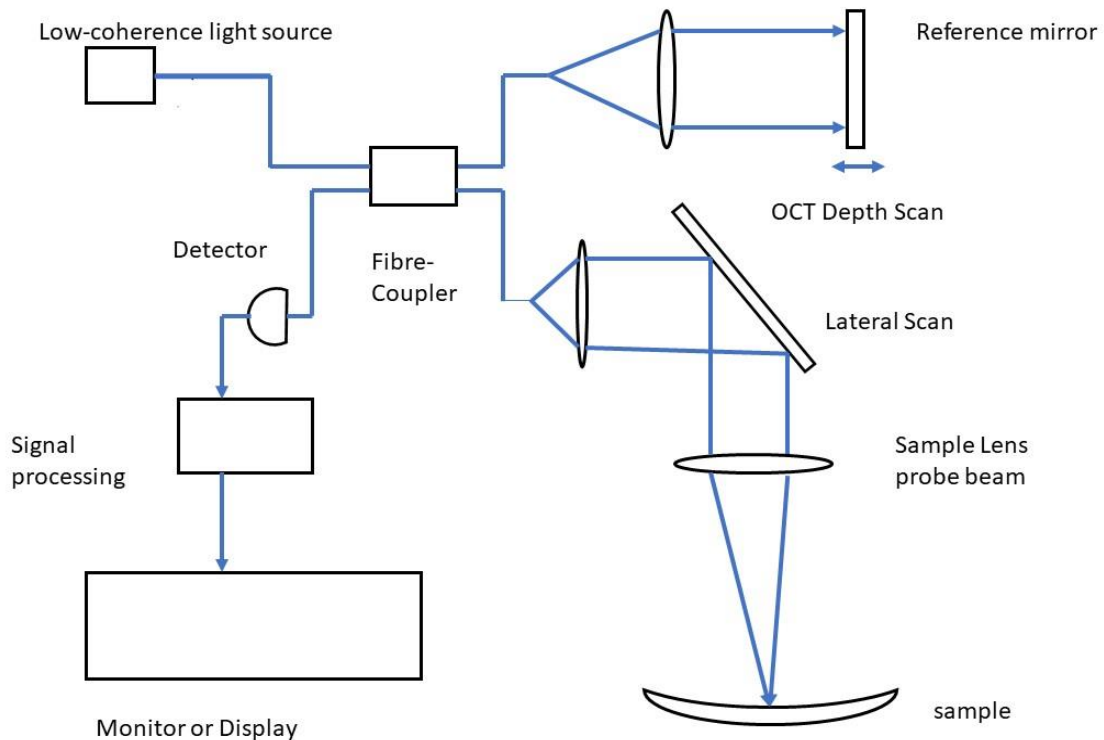
Figure 6 Fiber optics implementation of OCT(single mode)

2.3 Methods for performing OCT

Two methods are widely used for performing OCT, these include time domain OCT (TD-OCT) and frequency domain OCT (FD-OCT). Each of these methods have various advantages and disadvantages in imaging.

2.3.1Time domain OCT (TD-OCT)

In time domain OCT, the mirror in the reference arm of the interferometer is moved to match the delays in various layers of the sample. The resulting interference signal is processed to produce the axial scan waveform. Since the reference mirror must move one cycle for each axial scan, the need for mechanical movement limits the speed of image acquisition. In addition, at each moment, the detection system can collect only signals from a narrow range of the depth in the sample, therefore rendering the serial axial scanning inefficient.
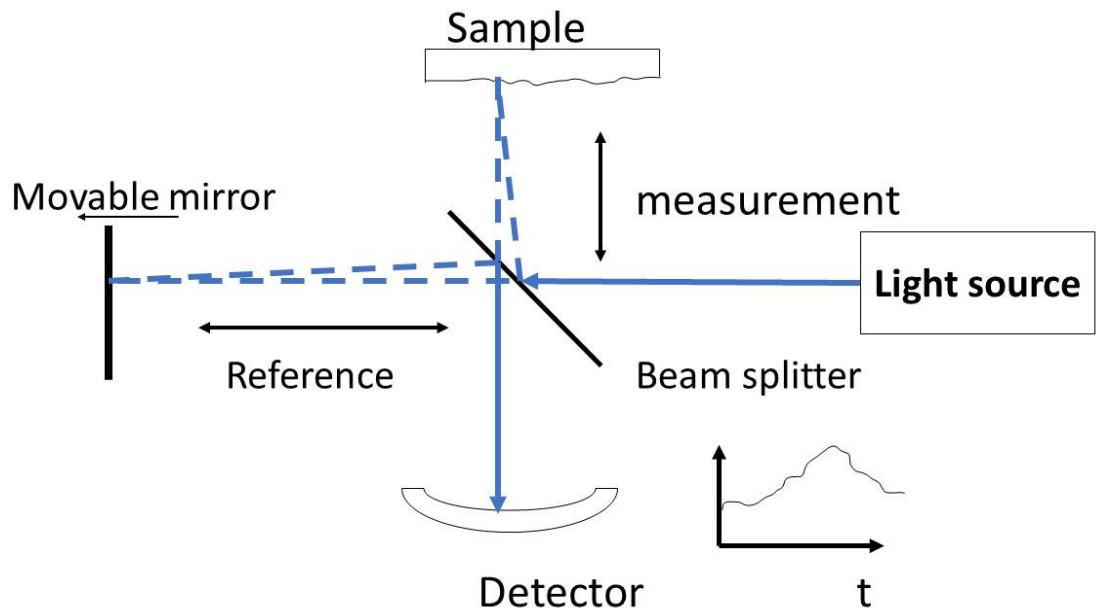
Figure 7 Principle of Time domain OCT

2.3.2 Frequency domain OCT (FD-OCT)

Even though the TD-OCT can be used to generate 1-dimensional or even 2-dimensional cross section of the sample, it usually involves translating the reference mirror longitudinally and scanning in order to obtain the image. Doing this requires a lot of time and will not be ideal for imaging large areas of the sample in real time. In FD-OCT, the reference mirror is kept constant and the spectral pattern of the interference between the reference and the sample reflections is measured. The spectral interferogram is Fourier transformed to produce an axial scan. The absence of any mechanical movements makes it possible for the image to be acquired very rapidly. Furthermore, reflections from all layers of the sample are detected simultaneously. The parallel axial scanning is much more efficient, resulting in both greater speed and higher signal-to-noise ratio. Frequency

18

domain OCT can be implemented in two ways: Spectral/Fourier domain OCT and swept

source domain OCT.

2.3.3 Fourier/Spectral domain OCT

In the spectral or Fourier domain OCT, a broad-spectrum light source is used, and a

spectrometer is utilized in the detector arm of the interferometer. The interfering light

enters the spectrometer and is spread into a spectrum. The spectrometer has a grating or

prism that spread the light into different beams based on the frequency or wavelength of

the light. The spectrum is detected by a linear detector.
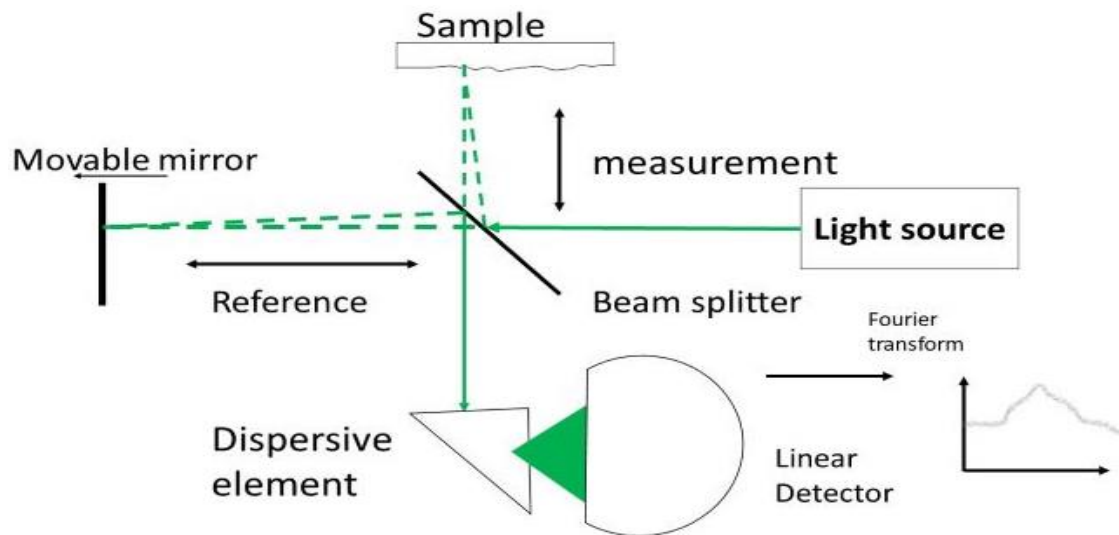
Figure 8 Principle of spectral domain OCT[18]

2.3.4 Swept Source domain OCT

In swept source domain OCT, a tunable laser is used to sequentially sweep through the

spectrum and the signal is collected by a photodetector. The advantage of sweep source

domain OCT using a photodetector over a linear detector is its ability to use a wide range

of wavelengths which are well suited for imaging scattering tissues, since there are less attenuations than in shorter wavelengths.[1]
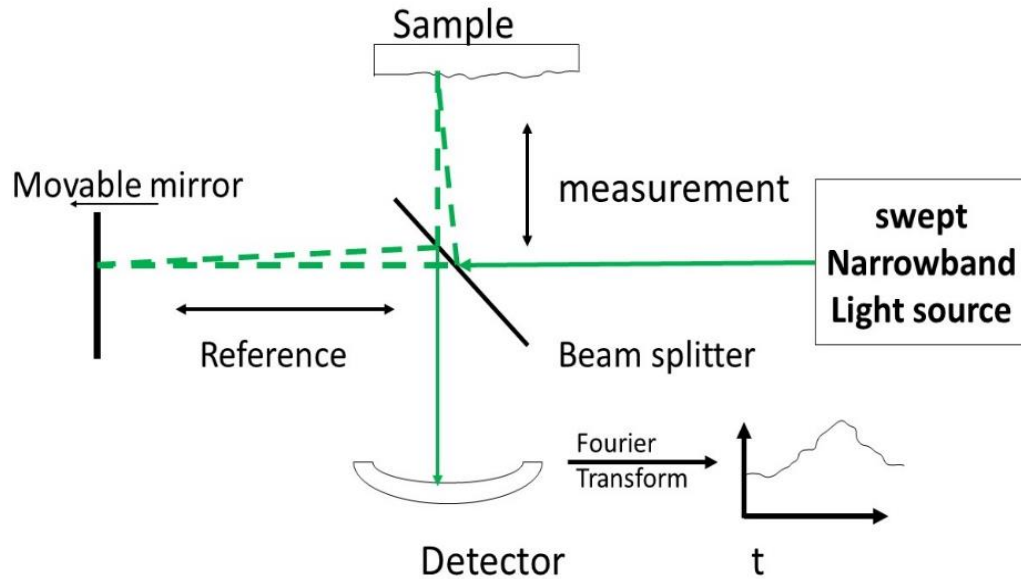
Figure 9 Principle of swept source domain OCT

2.4 Advantages and disadvantages of different methods

Spectral domain OCT has some advantages that makes it preferable for imaging biological tissues, these advantages include very high resolution and a reasonably high speed associated to spectral domain OCT since no mechanical movement of the parts is needed. Furthermore, the image produced using spectral domain OCT is highly visible, compared to that of TD-OCT.

The table below shows the relationship between spectral domain OCT and time domain OCT in terms of various characteristics:

Table 1 Comparison of Spectral domain OCT and Time domain OCT

[19][20][21][22]

Characteristics	Spectral domain OCT	Time domain OCT
Light source	840nm	820nm
Detector	Spectrometer	Single detector
Axial resolution	Same	Same
Transverse resolution	20 microns	20 microns
Scan depth	2mm	Limited by sampling can be in cm
Scan speed	About 200000 A scans per sec	1000 A scans per second
Signal to Noise Ratio	130dB	104dB
Sensitivity	Very high above 80dB	Very high

2.5 General Advantages of OCT for this study

In OCT technique for imaging, depth resolution is independent of the sample beam aperture and the coherence gate can substantially improve the probing depth scattering media. This makes OCT advantageous to other optical technique. Compared to non-optical imaging techniques, OCT has a very high depth and transverse resolution and can create function dependent image contrast. The main disadvantages of OCT compared to

alternative imaging modalities in medicine is its limited penetration depth in scattering media.

2.6 General applications of OCT Vibrometry

From its inception, OCT was initially applied to imaging in ophthalmology [23]. The advances in technology has made it possible for many applications in OCT to emerge, most of which are in the medical field[24]. OCT can be applied to various fields ranging from ophthalmology (Studies of the human eye) to dermatology (study of the skin)

OCT vibrometry in otology: OCT Vibrometry has been used by several scientists in Otology, to study normal and pathological anatomy and physiology of the ear.

R Wang et al used phased sensitive optical coherence tomography as a novel method, to image tissue of the organ of Corti at sub-nanometer scale. In this experiment, they deduced that biomechanical mechanisms of the response of the organ of Corti to sound could be measured using phase sensitive optical coherence tomography[25]

H Subhash et al applied OCT vibrometry technique to detect tiny motions of the middle ear structure such as the tympanic membrane, the ossicular chain and their morphological features for differential diagnostics of conductive hearing losses. They were able to measure vibrational motion of the ossicles with a vibration sensitivity of about 0.5nm.[26]

OCT vibrometry in gastroenterology and dermatology: OCT has been used to image and diagnose digestive track disorders in the human body. Gastroenterological OCT was first initiated and performed by Izatt et al[27], who showed that OCT and OCM can be used for high resolution and characterization of dense scattering tissues and demonstrated

their applications in imaging of gastrointestinal tissues in vitro. In dermatology, OCT has been used to diagnose various skin lesions like carcinomas[28][29][30]

OCT in Ophthalmology: Ophthalmology is still the domineering field for medical OCT for the reasons mentioned above. Recently OCT has been used in imaging microscale displacement related to mechanical properties within the relative transparent media of the cornea and lens[31]. OCT Vibrometry technique has been used to measure mechanical wave speed, dispersion and viscoelastic modulus of the cornea, properties that are very important in Ophthalmology[32] [33]

OCT vibrometry technique has also been utilized in various ways to visualize and measure sound-induced vibrations in intracochlear tissues of a mouse and other rodents. [34][35][36][37][38][39][40]

In recent years OCT has been applied in Dentistry to detected decayed teeth[41][42][43] and caries lesions[44]. In hemostatic therapy, OCT has been used for recording of cardiac flow dynamics in developmental biology[45] and other non-medical applications like nondestructive evaluation of paints and coating[46]

2.7 Speckle Variance

Speckle present in biological tissue imaging is due to the interference of light backscattered from the tissue. Besides its role as noise in coherent imaging, speckle is a carrier of information about the tissue microstructure. Speckle has become very useful in a series of measurement techniques, spanning from the field of medicine to engineering. [47]. Speckle has been applied in pharmacodynamic studies to evaluate the motility of parasites [48]. In OCT imaging, speckle cannot be avoided since it is embedded in the

OCT image and results in the degradation of the image quality. Speckle reduction is a very important aspect in imaging. Research on speckle reduction has been conducted by many scientists[49], though the results always end with a conclusion that speckle cannot be totally reduced in imaging, and if speckle is completely removed, then no information can be found regarding the tissue microstructure or object being imaged[50]–[52]. Speckle variance OCT, a specialized field in OCT has been used to study different physical phenomena; speckle variance OCT has been used to image the morphology *in vivo* of a mice[53] and has also been used for visualizing blood flow within human retinal capillary networks[54]

CHAPTER 3

MATERIALS AND METHODS

3.1 Instrumentation

Below is a list of all the instruments that were used in this research project with various specifications:

- Superluminescent Diode (SLD) with 920nm wavelength, 30nm bandwidth and 20mw optical power, forward voltage of 2.5V and forward current of 150mA

- Faraday Optical Isolator(FOI) with a center wavelength of 850nm, a spectral range of 840nm-960nm, a clear aperture of 4mm. It has an isolation of 30-38dB and a Dichroic glass polarizer.

- Cobra-S Spectrometer with a 920nm and 28-300nm bandwidths

- 3*3*2mm, 75V Piezo chip with wires

- Two Plano-Convex lenses with focal lengths of 12.5mm and 40mm

- Optics in motion beam stirring mirror with a 1" * 0.25" glass mirrors

- 930nm Fibre Optic coupler with ± 100nm Bandwidth, 50/50 split ratio and a signal output of 44.0% - 56%

- Various Mounts and drivers

- Kinematic mounts and 4mm mirrors

- Laser diode controller

- TEC Controller with output voltage and power of 4V and 4W respectively

- 26mm translational stage

- Function Generator

- Computer Interface

3.2 Production of a Spherical Laser Beam

The Light source used for our OCT system is an SLD because it has a high power, broad band spectrum and the emitted light has a short coherence length. An SLD is a combination of a laser diode and a light emitting diode (LED). Since the light beam produced by the SLD is elliptical in nature, the power output will be less efficient and it will be difficult coupling the elliptical beam into the optical fiber; therefore, the first thing we did was to produce a spherical beam of light from the elliptical beam. In order to do this, we used a silver coated reflective mirror to reflect the elliptical laser beam into a Faraday Optical Isolator (FOI) with a wavelength of 850nm and a center aperture of 4mm. The FOI allows the transmission of light in one direction only in order to prevent unwanted feedback or backscattering of light. The light then passes through two plano-convex lenses and is reflected into the optical fiber using a reflective mirror. A plano-convex lens is a converging lens with one flat surface and one convex surface that allows light to be focused, collected and collimated. In principle, parallel beam of light that leaves the FOI is brought to focus at the optical fiber using the two plano-convex lenses.
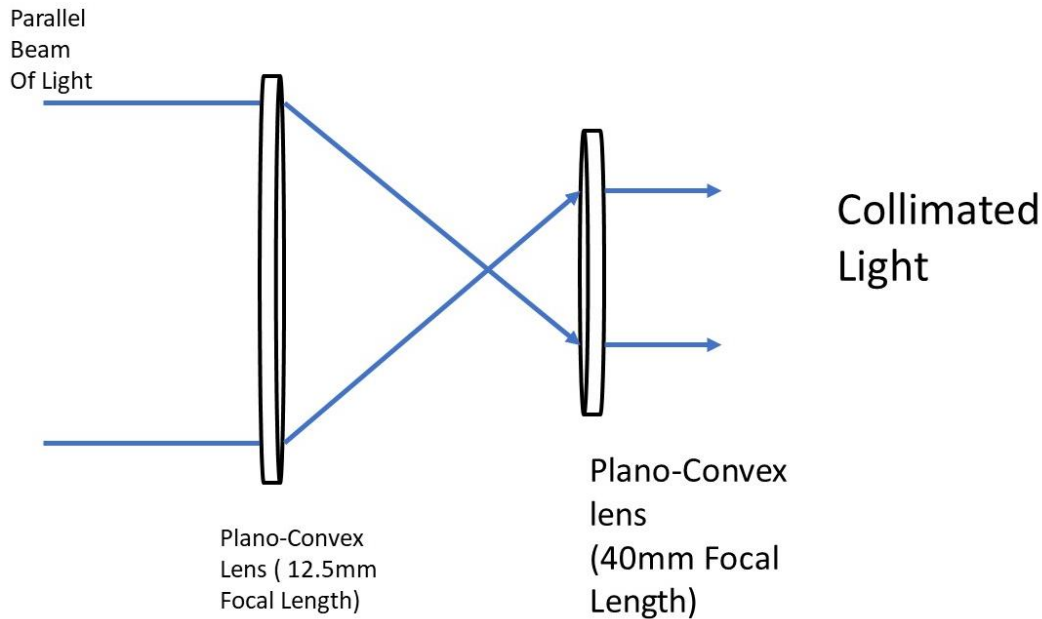
Figure 10 Plano-Convex Lens Combination

Since the two lenses are oriented in such a way that the light beams enter and exit the lenses through the curved (convex) surface, very low spherical aberration is achieved, hence the light beam that enter the optical fiber is spherical in shape, focus, and has a very high power. We can therefore expect very high image quality.

3.3 Layout of the Optical Fiber OCT System

Figure 8 below shows a layout of the OCT system used in this research. When all apparatus is put together and plugged into the power supply, light beam from the SLD is incident unto a reflective 4mm mirror M1 and M1 reflects the light rays into a FOI. The FOI allows light to be transmitted in one direction only and eradicates any backscattering of the light. The light beam leaving the FOI passes through 2 plano-convex lenses(PCL1 and PCL2) of different radii and focal lengths and is reflected by a reflective mirror (M2) into an optical Fibre system. The optical Fibre system has a 930nm Fibre optic coupler with ±

100nm Bandwidth and a 50/50 split ratio. The light rays that enter the Fiber optic coupler

is split into a 50/50 ratio, 50% of the light rays goes into the reference arm and the other

50% goes to the sample arm.
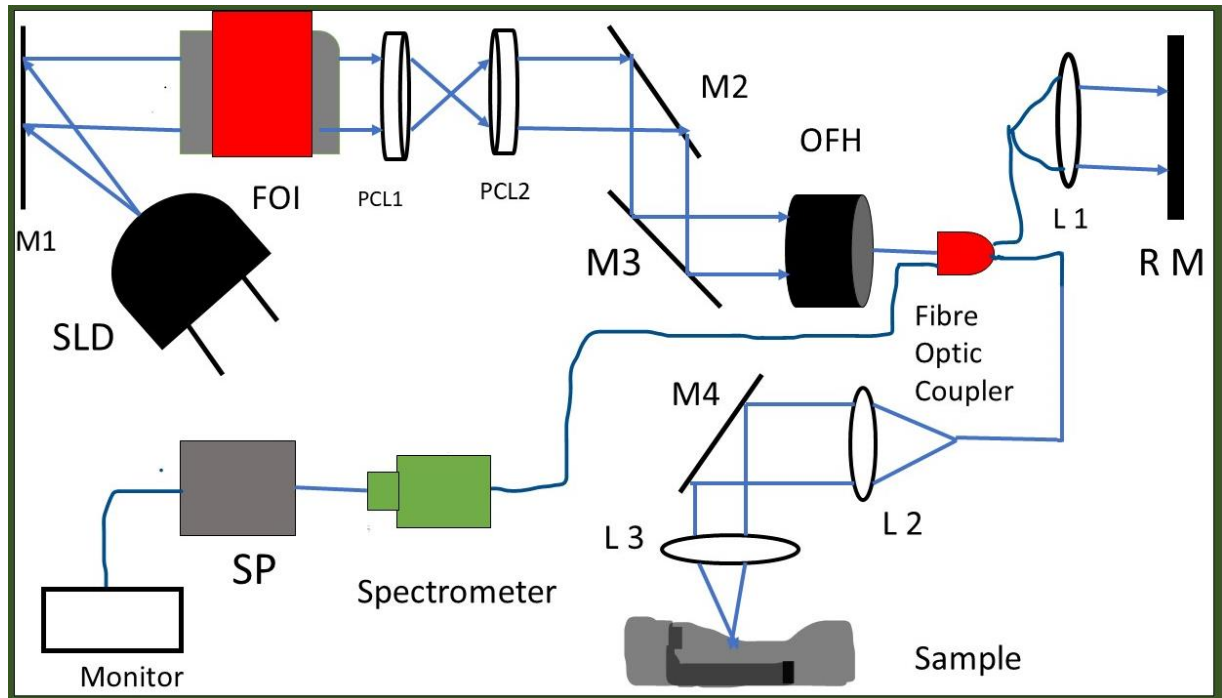
Figure 11 Schematic of a Fibre optic Fourier domain OCT system.
 SLD = Superluminescent Diode. FOI = Faraday Optical Isolator. PCL1 = Plano-Convex
Lens 1 (with 12.5mm focal length). PLC2 = Plano-Convex Lens (With 40mm Focal
length). M1, M2, M3 and M4 are silver coated reflective 4mm mirrors. OFH = Optical
Fibre Head. L1, L2 and L3 are Converging Lenses. RM = Reference Mirror and SP =
Signal processing.

The light rays that enter the reference arm are reflected back through the same path by

the reference mirror (RM) while some of the light rays is transmitted. The light rays that

enters the sample arm is converged unto a reflective mirror M4 using a converging lens

L2, and the rays are then incident into a test sample using another converging lens L3.

Some of the light rays that are incident on the sample are transmitted into the sample and

the other are reflected through the same path. The two reflected light; the one from the sample and the other from the reference mirror later recombine by the process of interference. Interference can either be constructive or destructive, depending on whether the two light sources started in phase or pi out of phase. For the case in which the two light beams started in phase, constructive interference will occur when the path difference between the two reflected light is zero or an integer number of wavelengths. In this case the two light beams(waves) combine perfectly creating an even larger wave, with peaks equal to two times the peak of one of the waves(light). Destructive interference occurs when the path difference between the two light beams(waves) equals half of an integer of wavelengths. In this case the two waves (light beams) cancel the effect of each other and we don't see anything at the detector.

The combined light beam(by constructive interference) is directed through a fiber optic cable into the spectrometer through a narrow aperture. The spectrometer has a prism or grating that disperses the spectral component of the light at slightly different angles. The spectral component of the light is then focused onto a detector. At the detector, the signal is processed using computer software and is displayed on a monitor.

3.4 Experiment 1: Measuring the DC Offset

In the first experiment, the sample arm is blocked using the black end of a Thorlabs detector card, and interferograms are collected. In this case, light rays leaving the SLD, get into the fiber optic cable and are split in a 50:50 ratio. The light that enters the reference arm is reflected by the reference mirror through the same path, while the light that enters

the sample arm is stopped from reaching the sample by an opaque object(Black card). At

the sample arm, there is no contact between the light rays and the test sample, therefore,

all the light rays reaching the detector are from the reference arm of the OCT system. The

light (signal) is processed using a software and is displayed on a monitor as interferograms.

This experiment is done multiple times to ensure accuracy.

3.5 Experiment 2: OCT system with piezo as the test sample

For the first part of experiment 2, a 3*3*2mm, 75V Piezo chip is placed on the objective

of the sample arm. The piezo is used as the vibrating source for this experiment. The first

part of the experiment is carried out without the piezo vibrating(no power). Light rays

entering the sample arm bounce off on the non-vibrating piezo and are reflected through

the same path and recombine with the reflected light from the reference arm at the

spectrometer and are detected by the detector. Using computer software, the signal is

processed and displayed on the monitor.

In the second part of the experiment, the piezo was powered using the function generator

at a frequency of 2500Hz. The piezo was placed at a horizontal surface (stage) oriented in

such a way that light rays emerging from the objective lens at the sample arm, strikes the

piezo at 90^0. Various measurements were taken at different voltages ranging from 0.1V to

5V.

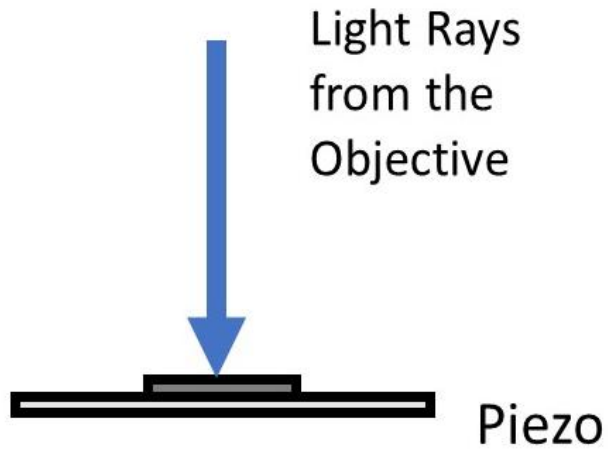Figure 12 Orientation of the Piezo 90^0 with respective to the Objective

The third part of experiment 2 was performed while the piezo was vibrating at a frequency of 2500Hz, the piezo was oriented in such a way that it made an angle of 85^0 with respect to the horizontal stage. Different measurements were taken at different voltages ranging from 0.1V to 5V.
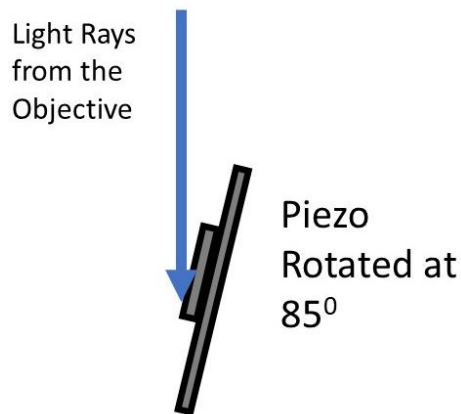

Figure 13 Piezo oriented at 85^0 to the Horizontal stage

In all these experiments the temperature of the SLD was kept in check using the TEC controller. If the temperature of the surrounding drops or increases to an undesired amount, the TEC controller stabilizes it at a room temperature of 25^0 C to ensure proper functioning of the SLD. All the experiments were repeated several times to ensure accuracy.

3.6 Mathematical Treatment of OCT

The OCT spectral interferogram can be written as

$$I(k) \alpha \, Re\{ \iint S(k)r(x,z) \exp\left(4ln2\left(\frac{x^2}{\omega_0}\right)\right) \exp(-i2kz)\, dxdz\} \tag{2}$$

Where $k=2\pi/\lambda$ denotes the wavelength, Re{} denotes the real part , operator, (x,z) denote the coordinate of the reference frame fixed to the sample, S(k) is the source power spectral density, r($x, z)$ is the backscattering coefficient of the sample and ω_0 is the full-width at half maximum of the beam intensity profile. For a Gaussian spectral shape

$$S(k)\alpha \, \exp(-4ln2(k-k_0)^2/\Delta k^2) \tag{3}$$

Equation (2) above can also be written also as

$$I(k) \propto S(k) \sum j\sqrt{R_{sj}R_r} \cos\{2nk\Delta z_j + 2nk_0 dz_j\} \tag{4}$$

Where $S(k)$ is the power spectrum of the light source represented by equation (2), R_{sj} is the reflectivity of the sample at the jth depth, R_r is the reflectivity of the reference arm, n is the refractive index between the reference and sample arm reflectors, k is the wavenumber, k_0 is the center wavenumber, Δz_j is the distance between the jth reflector in the sample and the reference reflector measured from traditional OCT and is defined by

the full width at half maximum of the spectrum source, and dz_j is the sub-resolution

displacements of the jth reflector in the sample, also interpreted as the phase shift.

The raw data acquired from the spectrometer is a pattern of light showing the intensity

as a function of wavelengths λ, an interpolation was done to obtain wave numbers ($k=2\pi/$

λ) as seen in equation (4). Taking the inverse Fourier transform of equation (4) yields a

complex signal in z-space

$$I(x) \propto \frac{1}{2}\gamma(z) \otimes \Sigma_i \sqrt{R_{si}R_r}\, \delta[z \pm 2n\Delta z]exp \pm 2njk_0dz \qquad (5)$$

where $\gamma(z)$, the coherence function is the FT of $S(k)$, $\otimes$ represents the convolution

operator, δ is the Dirac delta function and z is the position in depth within the sample.

Now for any given Δz, the phase of the signal is a linear function of dz, phase changes can

be tracked over time [55] . Equation (5) below can be used to convert the phase of the

interferogram to displacement

$$\mathbf{dz(2n\Delta z, t)} = \frac{1}{2nk_0}\big(< I(2n\Delta z, t) - < I(2n\Delta z, t_0)\big) \qquad (6)$$

CHAPTER 4 RESULTS AND CONCLUSION

Speckle is a very important concept in imaging biological tissues. Speckle is a property of the light source and the sample that remains unchanged under stable conditions . Any motion of the sample or the light source results in changes in speckle. As a result of the properties of speckle, we hypothesize that it is possible to detect small changes(vibrations) in the sample positions by tracking speckle over time.

Expected Results from Experiments

From all the experiments carried out using the powered piezo, we had certain expectations of what the results should be.

We expected the frequency domain phase signal that was **dependent** of Doppler angle since the phase of a signal is related to the angle. We also expected the frequency domain speckle signal to be **independent** of Doppler angle

Obtained Results from Experiments

To verify the accuracy of our experiments, we calibrated the vibrational motion of the piezo relative to the magnitude of the applied sinusoidal voltage. We found a linear relationship between measured piezo displacement and applied sinusoidal voltage.

We kept changing the sinusoidal voltage from 1mV to 5V, for each of the voltages we measured the piezo displacement using the OCT system and we found that increasing the voltage of the piezo using a function generator led to an increase in the displacements(vibrations) from the piezo. This was expected, since the function generator is the power house of the piezo, any increase in the voltage should lead to an increase in the piezo displacements, and any decrease in the voltage of the source(function generator)

34

should lead to a decrease in the piezo displacements. Figure 14 below further explains the results

displacement = 0.6962*voltage - 0.8911
$R^2 = 0.9999$
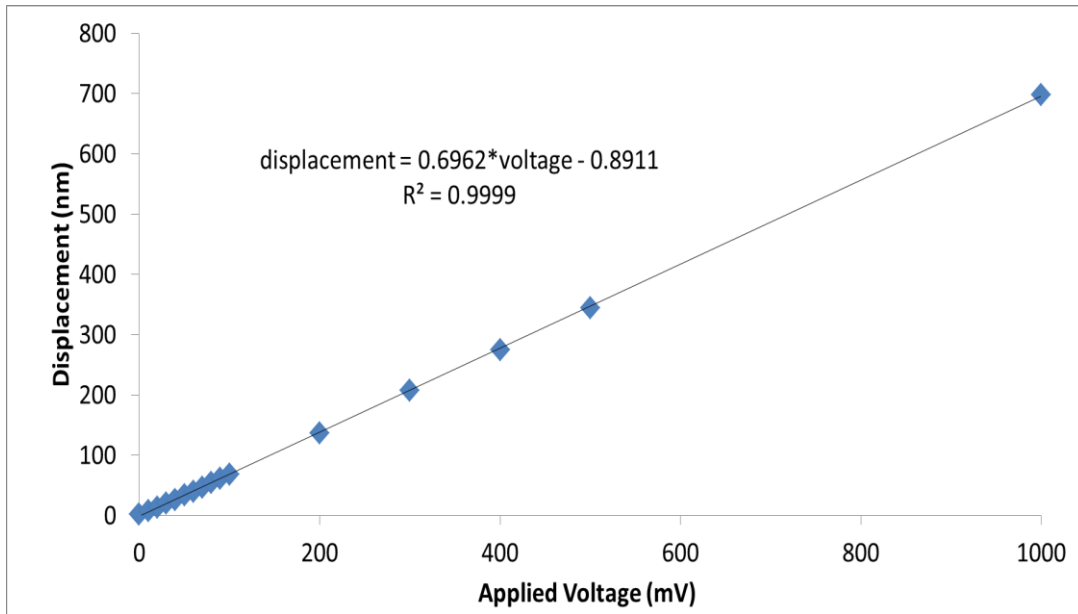
Figure 14 Graph of Displacement(nm) vs Applied Voltage(mV) for the piezo

Next, we characterized the dependence of the OCV signal to the Doppler angle of the imaging system. By rotating the axis of the beam relative to the vibrational direction of the piezo we characterized the loss in signal with Doppler angle. Surprisingly the loss of vibrational magnitude was not as pronounced as we expected, implying either displacement of the piezo in multiple axes or some compounding source of noise.

Figure 15 below shows a relationship between the displacements(in nanometers) from the piezo vs the Doppler angle(in degrees) for different voltages obtained from the **frequency domain phase signal.**
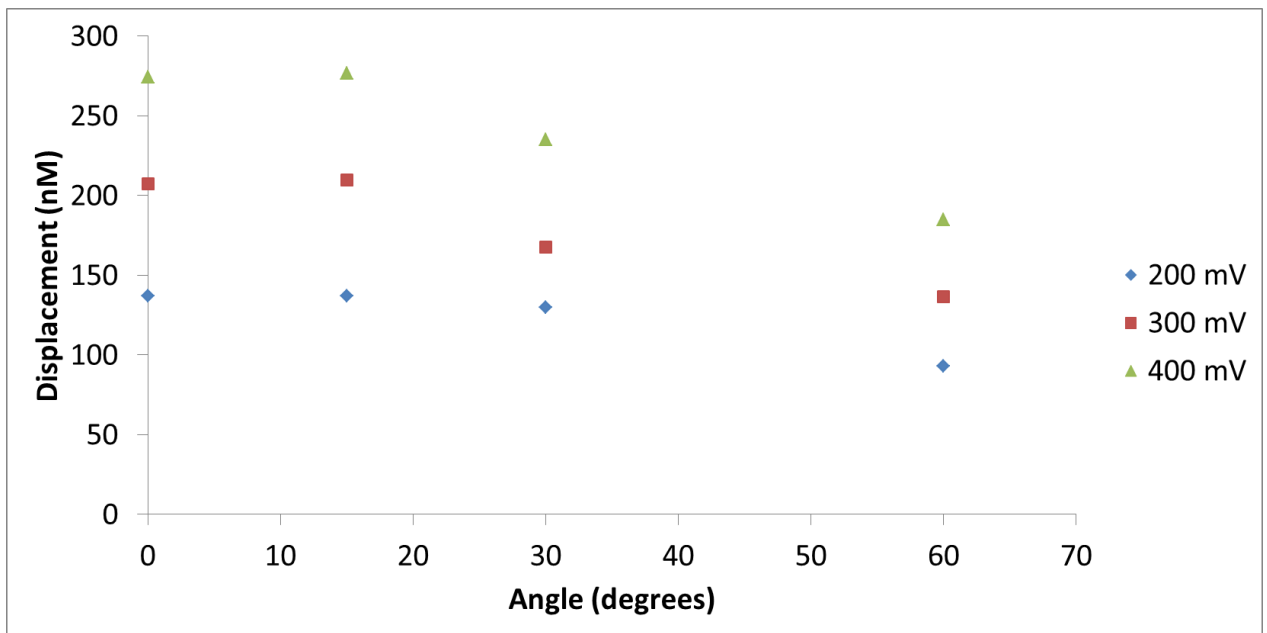
Figure 15 Graph of Displacement(nm) vs Angle(degrees) for frequency domain phase signal for different voltages

From the Figure 15 above we observe a change in the displacements with different angles. Considering a voltage of 200mV, when the angle was 0^0 the displacement was approximately 140nm, at an angle of 30^0 the displacement decreases to a value of 135nm and at angle of 60^0, the displacement was measured to be approximately 100nm. This was the same trend observed at a voltage of 300mV and 400mV. The data obtained from the frequency domain phase signal indicates a decrease in the measured displacements when the angle increase, **hence, we conclude that the frequency domain phase signal is dependent on Doppler angle.**

The data from frequency domain phase signal and speckle signal showed that speckle measurements can track vibrational motion with a lower sensitivity compared to phase signal (Figure 16) and frequency domain speckle signal is dependent on Doppler angle(Figure 17).
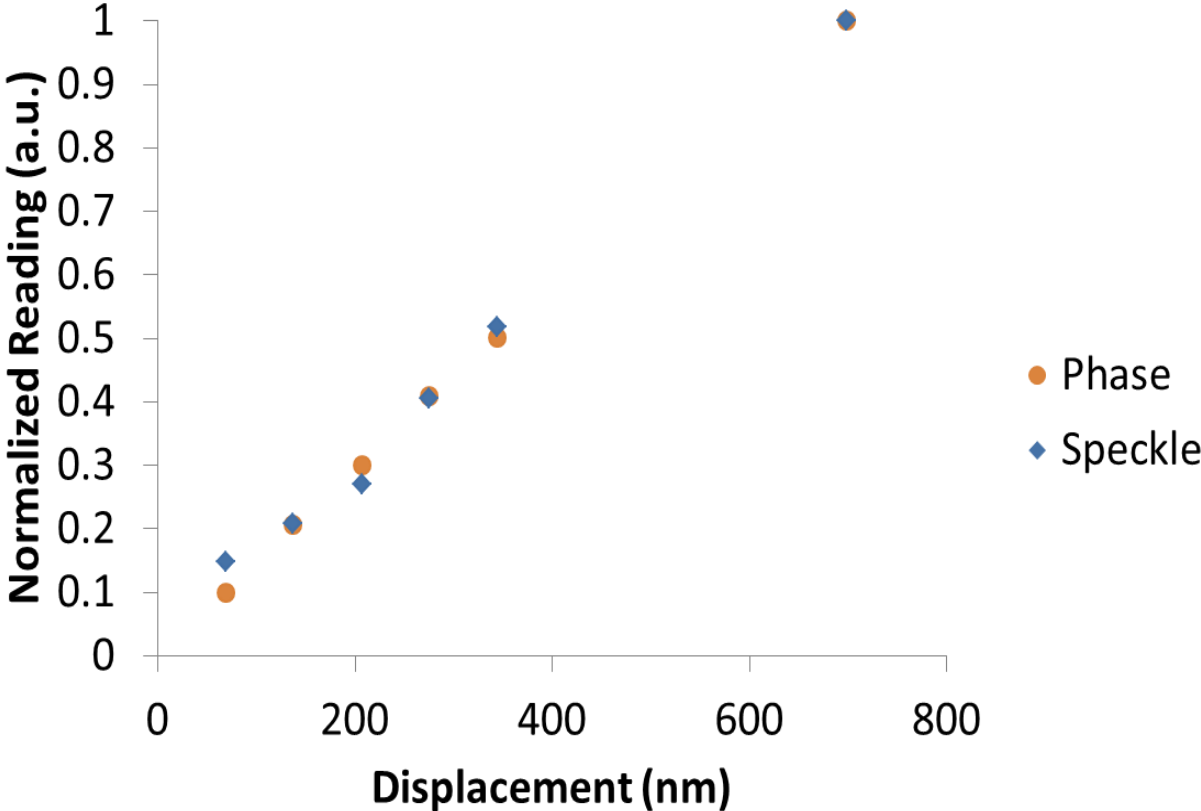
Figure 16 Sensitivity in vibrational measurements of Phase signal vs Speckle signal
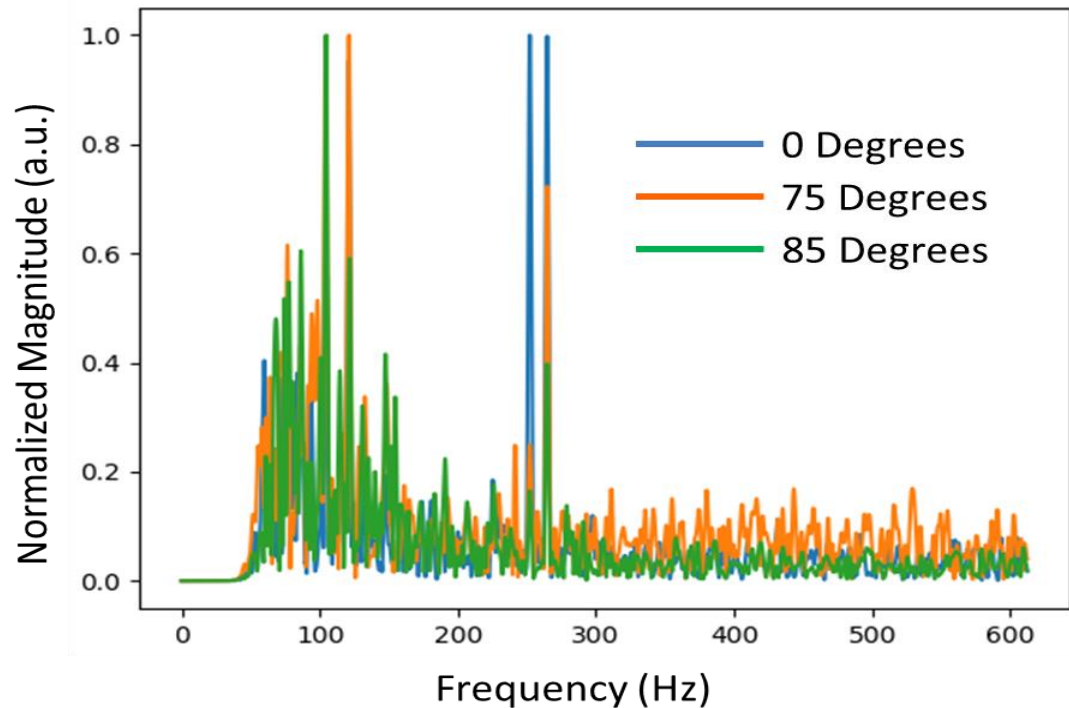
Figure 17 Graph of Normalized magnitude vs Frequency for speckle signal.

We didn't expect a dependency in Doppler angle using speckle. Some of the questions we have that may have resulted in this dependency may be related to the roughness of the surface or the impact of layered motion in speckle, since we looked at the single layer (surface) of the piezo. We used the decorrelation method and the FFT method and had the same results for speckle signal, so it is possible that our methods for extracting measurements were wrong.

Accomplished task

We were able to build and assemble an OCT system that can collect nanometer scale vibrational motion.
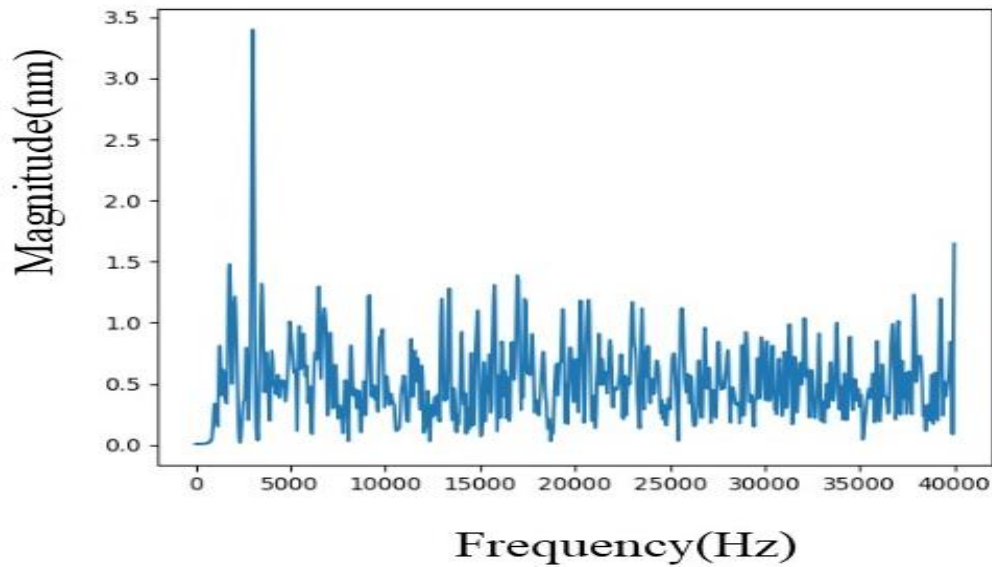
Figure 18 Graph of Magnitude(nm) vs Frequency(Hz) of spectral interferogram from OCT system.

Conclusion

We have performed an initial characterization of the vibrational sensitivity of speckle variance OCT. From our measurements, we determined a based sensitivity of speckle variance OCT of 50 nm vibrational motion with a signal to noise ratio of 1.7 dB. For the same vibrational motion, we measured a signal to noise ratio of 39.4 dB from phase variance. Contrary to our expectations, we found that both speckle variance measurements of vibration and phase variance measurements of vibration were highly dependent upon the Doppler angle. Thus, while there is potential for speckle variance OCT to detect nanometer scale vibrational motion, further work must be performed to determine if it is indeed possible to decouple speckle variance from the Doppler angle. If future work

determines it is impossible to decouple speckle from the Doppler angle, phase variance is a far more powerful technique.

Recommendation for Further Research

Our results showed a dependency of frequency domain speckle signal on Doppler angle. This was not supposed to be the case, so part of the work than can be done in the future will be to repeat the experiments using the high-speed OCT system and to verify why this dependency exists. Next, a relationship between the roughness of the sample and speckle (speckle decorrelation) must be determined, since our experiment did not consider the roughness of the sample surface.

In addition, the impact on layered motion must be determined. A question that will need to be answered might be this: what role does movement above the sample play on the sample itself? Finally, a robust formula for converting speckle decorrelation measurements to vibrational magnitude must be determined.

REFERENCES

[1] J. G. Fujimoto and W. Drexler, "Introduction to OCT," in *Optical Coherence Tomography: Technology and Applications, Second Edition*, Springer International Publishing, 2015, pp. 3–64.

[2] J. I. Lane, E. P. Lindell, R. J. Witte, D. R. Delone, and C. L. W. Driscoll, "Middle and inner ear: Improved depiction with multiplanar reconstruction of volumetric CT data," *Radiographics*, vol. 26, no. 1, pp. 115–124, 2006.

[3] C. Czerny, W. Gstoettner, P. Franz, W. D. Baumgartner, and H. Imhof, "CT and MR imaging of acquired abnormalities of the inner ear and cerebellopontine angle," *Eur. J. Radiol.*, vol. 40, no. 2, pp. 105–112, 2001.

[4] B. Teele, David W, Klein Jerome O, Rosner, "Epidemiology of Otitis Media during the First Seven Years of Life in Children in Greater Boston : A Prospective , Cohort Study Author (s): David W . Teele , Jerome O . Klein , Bernard Rosner and Greater Boston Otitis Media Study Group Published by : Oxf," *J. Infect. Dis.*, vol. 160, no. 1, pp. 83–94, 1989.

[5] D. L. Blackwell, J. W. Lucas, and T. C. Clarke, "Summary health statistics for U.S. adults: national health interview survey, 2012.," *Vital Health Stat. 10.*, no. 260, pp. 1–161, 2014.

[6] R. L. Goode, G. Ball, S. Nishihara, and K. Nakamura, "Laser Doppler vibrometer (LDV)--a new clinical tool for the otologist.," *Am. J. Otol.*, vol. 17, no. 6, pp. 813–22, Nov. 1996.

[7] N. Stasche, H. J. Foth, K. Hörmann, A. Baker, and C. Huthoff, "Middle ear

transmission disorders-tympanic membrane vibration analysis by laser-doppler-vibrometry," *Acta Otolaryngol.*, vol. 114, no. 1, pp. 59–63, 1994.

[8]   J. J. Rosowski, R. P. Mehta, and S. N. Merchant, "Diagnostic utility of laser-Doppler vibrometry in conductive hearing loss with normal tympanic membrane.," *Otol. Neurotol.*, vol. 24, no. 2, pp. 165–75, Mar. 2003.

[9]   A. L. Nuttall, D. F. Dolan, and G. Avinash, "Laser Doppler velocimetry of basilar membrane vibration," *Hear. Res.*, vol. 51, no. 2, pp. 203–213, 1991.

[10]   S. Terasaki, N. Wada, N. Sakurai, N. Muramatsu, R. Yamamoto, and D. J. Nevins, "Nondestructive Measurement of Kiwifruit Ripeness Using a Laser Doppler Vibrometer," *Trans. ASAE*, vol. 44, no. 1, pp. 81–87, 2001.

[11]   G. Binnig, C. F. Quate, and C. Gerber, "Atomi Force Microscope (invention)," *Phys. Rev. Lett.*, vol. 56, no. 9, pp. 930–934, 1986.

[12]   G. M. McClelland, R. Erlandsson, and S. Chiang, "Atomic Force Microscopy: General Principles and a New Implementation," in *Review of Progress in Quantitative Nondestructive Evaluation*, Springer US, 1987, pp. 1307–1314.

[13]   R. Hiesgen and K. A. Friedrich, "Atomic force microscopy," *PEM Fuel Cell Diagnostic Tools*, no. October, pp. 395–421, 2011.

[14]   S. Sikdar *et al.*, "Ultrasonic Doppler Vibrometry: Novel Method for Detection of Left Ventricular Wall Vibrations Caused by Poststenotic Coronary Flow," *J. Am. Soc. Echocardiogr.*, vol. 20, no. 12, pp. 1386–1392, Dec. 2007.

[15]   S. Sikdar, K. W. Beach, S. L. Goldberg, M. S. Lidstrom, and Y. Kim, "Ultrasonic doppler vibrometry: Measurement of left ventricular wall vibrations associated

with coronary artery disease," in *Annual International Conference of the IEEE Engineering in Medicine and Biology - Proceedings*, 2006, pp. 863–866.

[16] A. Mehmood, J. M. Sabatier, M. Bradley, and A. Ekimov, "Extraction of the velocity of walking human's body segments using ultrasonic Doppler," *J. Acoust. Soc. Am.*, vol. 128, no. 5, pp. EL316–EL322, Nov. 2010.

[17] A. Ekimov and J. M. Sabatier, "Human motion analyses using footstep ultrasound and Doppler ultrasound," *J. Acoust. Soc. Am.*, vol. 123, no. 6, pp. EL149–EL154, Jun. 2008.

[18] J. F. D. Boer, "Spectral/fourier domain optical coherence tomography," in *Optical Coherence Tomography: Technology and Applications, Second Edition*, Springer International Publishing, 2015, pp. 165–193.

[19] J. F. de Boer, B. Cense, B. H. Park, M. C. Pierce, G. J. Tearney, and B. E. Bouma, "Improved signal-to-noise ratio in spectral-domain compared with time-domain optical coherence tomography," *Opt. Lett.*, vol. 28, no. 21, p. 2067, 2003.

[20] R. Leitgeb, C. Hitzenberger, and A. Fercher, "Performance of fourier domain vs time domain optical coherence tomography," *Opt. Express*, vol. 11, no. 8, p. 889, 2003.

[21] N. Nassif *et al.*, "In vivo human retinal imaging by ultrahigh-speed spectral domain optical coherence tomography," *Opt. Lett.*, vol. 29, no. 5, p. 480, 2004.

[22] N. C. Lin, C. P. Hendon, and E. S. Olson, "Signal competition in optical coherence tomography and its relevance for cochlear vibrometry," *J. Acoust. Soc. Am.*, vol. 141, no. 1, pp. 395–405, 2017.

[23] J. A. Izatt *et al.*, "<title>Ophthalmic diagnostics using optical coherence tomography</title>," *Ophthalmic Technol. III*, vol. 1877, no. June 1993, pp. 136–144, 1993.

[24] D. Huang *et al.*, "Optical coherence tomography," *Science (80-.).*, vol. 254, no. 5035, pp. 1178–1181, Nov. 1991.

[25] R. K. Wang and A. L. Nuttall, "Phase-sensitive optical coherence tomography imaging of the tissue motion within the organ of Corti at a subnanometer scale: a preliminary study," *J. Biomed. Opt.*, vol. 15, no. 5, p. 056005, 2010.

[26] H. M. Subhash, A. Nguyen-Huynh, R. K. Wang, S. L. Jacques, N. Choudhury, and A. L. Nuttall, "Feasibility of spectral-domain phase-sensitive optical coherence tomography for middle ear vibrometry," *J. Biomed. Opt.*, vol. 17, no. 6, p. 060505, 2012.

[27] J. A. Izatt, M. D. Kulkarni, H. W. Wang, K. Kobayashi, and M. V. Sivak, "Optical coherence tomography and microscopy in gastrointestinal tissues," *IEEE J. Sel. Top. Quantum Electron.*, vol. 2, no. 4, pp. 1017–1028, 1996.

[28] J. Welzel, E. Lankenau, R. Birngruber, and R. Engelhardt, "Optical coherence tomography of the human skin," *J. Am. Acad. Dermatol.*, vol. 37, no. 6, pp. 958–963, 1997.

[29] J. Welzel, "Optical coherence tomography in dermatology: a review," *Ski. Res. Technol.*, vol. 7, no. 1, pp. 1–9, Feb. 2001.

[30] M. C. Pierce, J. Strasswimmer, B. H. Park, B. Cense, and J. F. De Boer, "Advances in optical coherence tomography imaging for dermatology," *J. Invest.*

Dermatol., vol. 123, no. 3, pp. 458–463, 2004.

[31] M. A. Kirby *et al.*, "Optical coherence elastography in ophthalmology," *J. Biomed. Opt.*, vol. 22, no. 12, p. 1, Dec. 2017.

[32] A. Ramier, B. Tavakol, and S.-H. Yun, "Measuring mechanical wave speed, dispersion, and viscoelastic modulus of the cornea using optical coherence elastography," *Opt. Express*, vol. 27, no. 12, p. 16635, Jun. 2019.

[33] Z. Han *et al.*, "Optical coherence elastography assessment of corneal viscoelasticity with a modified Rayleigh-Lamb wave model," *J. Mech. Behav. Biomed. Mater.*, vol. 66, pp. 87–94, Feb. 2017.

[34] J. J. Rosowski, M. E. Ravicz, S. W. Teoh, and D. Flandermeyer, "Measurements of middle-ear function in the Mongolian gerbil, a specialized mammalian ear," *Audiol. Neuro-Otology*, vol. 4, no. 3–4, pp. 129–136, May 1999.

[35] S. S. Gao *et al.*, "Vibration of the organ of Corti within the cochlear apex in mice," *J. Neurophysiol.*, vol. 112, no. 5, pp. 1192–1204, Sep. 2014.

[36] B. E. Applegate, R. L. Shelton, S. S. Gao, and J. S. Oghalai, "Imaging high-frequency periodic motion in the mouse ear with coherently interleaved optical coherence tomography," *Opt. Lett.*, vol. 36, no. 23, p. 4716, Dec. 2011.

[37] J. S. Iyer *et al.*, "Micro-optical coherence tomography of the mammalian cochlea," *Sci. Rep.*, vol. 6, Sep. 2016.

[38] W. Dong, A. Ia, P. D. Raphael, S. Puria, B. Applegate, and J. S. Oghalai, "Organ of corti vibration within the intact gerbil cochlea measured by volumetric optical coherence tomography and vibrometry," *J. Neurophysiol.*, vol. 120, no. 6, pp.

2847–2857, Dec. 2018.

[39] H. M. Subhash, V. Davila, H. Sun, A. T. Nguyen-Huynh, A. L. Nuttall, and R. K. Wang, "Volumetric in vivo imaging of intracochlear microstructures in mice by high-speed spectral domain optical coherence tomography," *J. Biomed. Opt.*, vol. 15, no. 3, p. 036024, 2010.

[40] Z. Jawadi, B. E. Applegate, and J. S. Oghalai, "Optical coherence tomography to measure sound-induced motions within the mouse organ of Corti in vivo," in *Methods in Molecular Biology*, vol. 1427, Humana Press Inc., 2016, pp. 449–462.

[41] A. Baumgartner *et al.*, "Polarization-Sensitive Optical Coherence Tomography of Dental Structures," *Caries Res.*, vol. 34, no. 1, pp. 59–69, 2000.

[42] R. Brandenburg, B. Haller, and C. Hauger, "Real-time in vivo imaging of dental tissue by means of optical coherence tomography (OCT)," *Opt. Commun.*, vol. 227, no. 4–6, pp. 203–211, Nov. 2003.

[43] A. Baumgartner *et al.*, "Optical coherence tomography of dental structures," in *Lasers in Dentistry IV*, 1998, vol. 3248, p. 130.

[44] D. Fried, J. Xie, S. Shafi, J. D. B. Featherstone, T. Breunig, and C. Q. Le, "Imaging caries lesions and lesion progression with polarization-sensitive optical coherence tomography," in *Lasers in Dentistry VIII*, 2002, vol. 4610, p. 113.

[45] S. Yazdanfar, M. D. Kulkarni, and J. A. Izatt, "High resolution imaging of in vivo cardiac dynamics using color Doppler optical coherence tomography," *Opt. Express*, vol. 1, no. 13, p. 424, Dec. 1997.

[46] F. Xu, H. E. Pudavar, P. N. Prasad, and D. Dickensheets, "Confocal enhanced

optical coherence tomography for nondestructive evaluation of paints and coatings," *Opt. Lett.*, vol. 24, no. 24, p. 1808, Dec. 1999.

[47] P. K. Rastogi, "Measurement of in-plane strains using electronic speckle and electronic speckle-shearing pattern interferometry," *J. Mod. Opt.*, vol. 43, no. 8, pp. 1577–1581, 1996.

[48] J. A. Pomarico *et al.*, "Speckle interferometry applied to pharmacodynamic studies: Evaluation of parasite motility," *Eur. Biophys. J.*, vol. 33, no. 8, pp. 694–699, Dec. 2004.

[49] M. Bashkansky and J. Reintjes, "Statistics and reduction of speckle in optical coherence tomography," *Opt. Lett.*, vol. 25, no. 8, p. 545, Apr. 2000.

[50] K. W. Gossage *et al.*, "Texture analysis of speckle in optical coherence tomography images of tissue phantoms," *Phys. Med. Biol.*, vol. 51, no. 6, pp. 1563–1575, Mar. 2006.

[51] Z. Li, H. Li, Y. He, S. Cai, and S. Xie, "A model of speckle contrast in optical coherence tomography for characterizing the scattering coefficient of homogenous tissues.," *Phys. Med. Biol.*, vol. 53, no. 20, pp. 5859–5866, 2008.

[52] J. M. Schmitt, S. H. Xiang, and K. M. Yung, "Speckle in optical coherence tomography: an overview," 1999, p. 450.

[53] O. Liba *et al.*, "Speckle-modulating optical coherence tomography in living mice and humans," *Nat. Commun.*, vol. 8, Jun. 2017.

[54] H. C. Hendargo, R. Estrada, S. J. Chiu, C. Tomasi, S. Farsiu, and J. A. Izatt, "Automated non-rigid registration and mosaicing for robust imaging of distinct

retinal capillary beds using speckle variance optical coherence tomography," *Biomed. Opt. Express*, vol. 4, no. 6, p. 803, Jun. 2013.

[55] H. C. Hendargo, A. K. Ellerbee, and J. A. Izatt, "Spectral domain phase microscopy," *Springer Ser. Surf. Sci.*, vol. 46, no. 1, pp. 199–228, 2011.